ISSN: 2278 – 7798
International Journal of Science, Engineering and Technology Research (IJSETR)
Volume 2, Issue 7, July 2013

Performance analysis of minimum volume based geometrical approaches for spectral unmixing

Bijitha.S.R, Geetha. P,Nidhin Prabhakar.T.V, Soman.K.P
Centre for Excellence In Computational Engineering And Networking,
Amrita Vishwa Vidyapeetham, Ettimadai, Coimbatore-641112

***Abstract*— Hyperspectral imaging is an area of interesting researches in the current scenario. The HSC(Hyperspectral cameras) used in this field is having high spectral resolution and low spatial resolution and by this reason, the spectra of pixels in the acquired data will appear as mixtures of spectra of various endmembers present in that area. Here spectral unmixing comes as a major process in the hyperspectral image analysis part. Spectral unmixing is a process by which user gets the number of pure reference materials called (endmembers),their spectral signatures and their corresponding abundance maps from y\the acquired hyperspectral data.In this paper performance analysis of three minimum volume based geometrical approaches namely MVSA(Minimum volume simplex analysis),MVES(Minimum volume enclosing simplex),and SISAL(simplex identification via split and augmented lagrangian) are done by applying them on the real hyperspectral data set AVIRIS Cuprite,taken over Nevada,U.S and the results are evaluated with reference to U.S.G.S spectral library which is available online.**

***Index Terms*—Hyperspectral imaging, MVES, MVSA, SISAL, Spectral signature, unmixing**

I. INTRODUCTION

Hyperspectral research plays a vital role in many fields as agriculture, military etc in the present scenario[1]. Hyperspectral remote sensing mainly works with the help of sensors as AVIRIS,ASTER etc, which are used to collect the information about an area of interest. Unlike multispectral sensors, these sensors collects the data in a large number of narrow and contiguous spectral bands ,which covers not only visible region of the spectrum but also the near and short infrared regions of the electromagnetic spectrum[2],[28] . Thus it is capable of providing much information about the observed scene than multispectral sensors. AVIRIS of NASA is having about 224 spectral channels and able to cover the wavelength region of 0.3-2.5µm[3].These sensors are having high spectral resolution, but the spatial resolution is limited, and due to this the pixels in the acquired image may comprise information of multiple endmembers present in the scene,and thus the spectra of pixels will be the mixtures of spectra of many materials,and thus the analysis comes as a tough task.Then spectral unmixing comes as an unavoidable process in this situation[4].

Spectral unmixing appears as a source separation problem

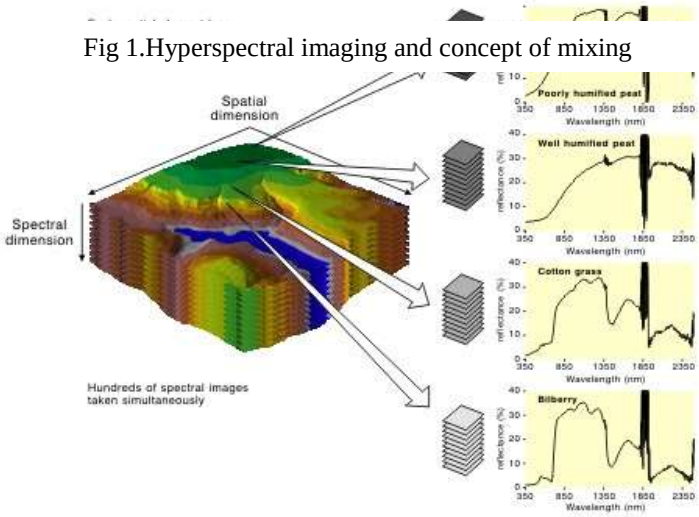

Fig 1.Hyperspectral imaging and concept of mixing

in the hyperspectral image analysis. This recovers the endmember spectral signatures and corresponding abundance maps from the highly mixed hyperspectral data sets acquired . The figure shown in fig1[5],shows the concept of hyperspectral imagery and from this we can understand that each pixel spectra is a combination of many material spectra and this indicates the need of spectral unmixing.

A. Concept of Spectral unmixing

As stated earlier, in hyperspectral imaging and analysis spectral unmixing plays an important role. This appears as a blind source separation problem in this case of hyperspectral imaging. The sources in the hyperspectral images may combine either in a linear or nonlinear mode and these sources may be statistically dependent in most of the cases. Thus the problem of spectral unmixing becomes more complex.

Spectral unmixing decomposes the acquired pixel spectra in to individual endmember spectra and also generates corresponding abundance maps of each pure reference material(endmember) and makes the analysis of acquired data easier[4].This unmixing models can be broadly classified in to two types.They are linear models[6] and nonlinear models[7].This can be explained with the help of figures shown in Fig2[8] and Fig 3[8].

Linear models starts with an assumption that the light that incidents on the area of interest makes an interaction with only one material and the scale of mixing is macroscopic[6].In this

case only single scattering occurs,and this is popularly used .

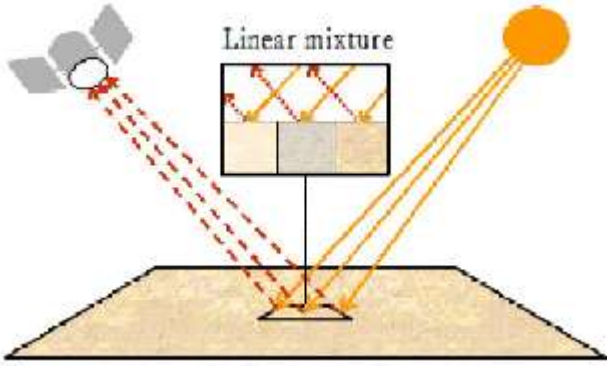

Fig.2 Linear model with single scattering effects.

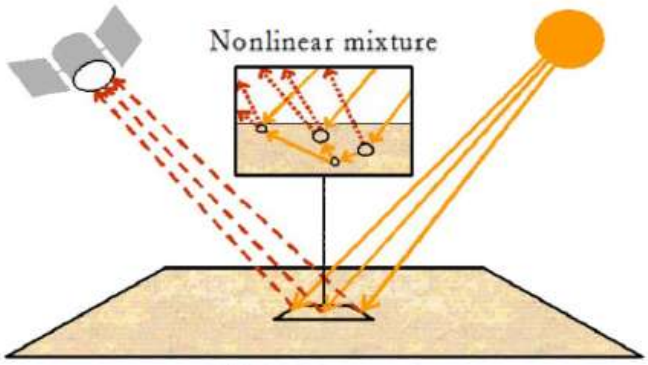

Fig 3.Nonlinear model with multiple scatterings

According to the Nonlinear model[7] shown in Fig 3 ,the light incident on the surface is scattered by multiple materials and this makes the observed model more complicated and this leads to microscopic level interaction and spectral unmixing according to this model is also becomes complicated. So most of the spectral unmixing algorithms works on the basis of linear model which is explained in the following section.

B.Linear Model-Mathematical Background

The linear mixing model makes an initial assumption that the spectra of a pixel in the observed scene is a linear combination of all pure reference materials (endmembers) and formed in a linear way as shown in fig 2. It is taken that the hyperspectral sensor used for covering the scene has L spectral channels or bands ,then the linear mixing model can be mathematically expressed as follows as in [8].

$$y = M\alpha + n \qquad (1)$$

Where y is an Lx1 column vector ,M is an Lxq matrix containing q endmembers(pure reference materials) of the scene and α is a qx1 vector containing the fractional abundances of the endmembers in the observed pixel and n is another Lx1 vector indicating the errors in the measurement that affect the calculations made at each pixel[8].In this model both matrices M and α have to be estimated by spectral unmixing. Here ANC (abundance non-negativity constraint) $\alpha_i \geq 0$,where i=1,2….q and ASC(abundance sum to one constraint), $1^T \alpha = 1$ are satisfied. This takes in to account another important fact into consideration that α_i ,for i=1,2…q ,represent the proportions of the pure reference materials or endmembers present in the scene. In this $Y \equiv \{y_i \in R^L, i = 1,...n\}$ of n number. of observed vectors with dimension L.

C.Summary Of Endmember Extraction Algorithms

Spectral unmixing algorithms are mainly get classified in to 3 categories as statistical,Sparse based and geometrical based unmixing algorithms. An overall summary to these approaches is given in this part.

Statistical approaches is the first category which [9] are formed on a Bayesian framework. Due to reason of high computational complexity of statistical approacheswhen compared with other unmixing approaches ,it's rarely used for unmixing purposes. Statistical dependence of sources are taken in to account in this case of statistical approaches .Here ICA[10](independentcomponentanalysis),DECA[11](Dependent component analysis) etc are examples of some common algorithms coming under this group .

The second type of algorithms comes under sparse based approaches[9].In this endmember extraction problem is formulated in a semisupervised fashion and it's assumed that the observed spectral signatures can be expressed as a linear combination of known spectral signatures from a library which contains ideal spectral signatures as U.S.G.S library. The examples of these algorithms coming under this set are SUNSAL[8],OMP[8],ISMA[8],and SUNSAL-TV[12]. This is a recently developed approach in the case of spectral unmixing and is a very efficient means for solving the problem.

Geometrical approaches[9] is the third group of spectral unmixing algorithms. In this the basic assumption is made as if works under linear mixing model, the spectral vectors of the dataset comes under a simplex, whose vertices correspond to pure reference materials(endmembers) and thus determines their spectral signatures .

These are most popularly used spectral unmixing algorithms. In this again it is subdivided into 2 sub classes. They are pure pixel based approaches and minimum volume based approaches.

Pure pixel based algorithms assume the presence of at least one pure pixel per endmember and cannot work if this assumption is violated.VCA [16](vertex component analysis), AVMAX [13] (Alternating volume maximization), SVMAX[13] (Successive volume maximization), ADVMM[14](Alternating decoupled volume max-min), SDVMM[14](Successive decoupled volume max-min), N-finder[15]etc are the important examples for this algorithm.

But in all cases these kind of pure pixels are not available in the observed scene ,and then we go for minimum volume based algorithms which do not need the assumption of pure pixels. The examples for this type are MVSA[17], MVES[18] and SISAL[19] .

In this paper the performance evaluation and comparative study the following algorithms namely SISAL, MVSA, and

MVES is done after applying on real hyperspectral data set Cuprite taken over Nevada ,U.S in 1997[20].

The rest of the paper is organized as follows. section 2 gives a brief theoretical and mathematical overview of algorithms employed, section 3 shows the experimental results and performance analysis. Section 4 draws the conclusion of the work done which is followed by references.

II. MINIMUM VOLUME BASED ALGORITHMS

In this a brief overview of the three geometrical approaches used for spectral unmixing is given .The three approaches namely MVSA,MVES and SISAL are minimum volume based algorithms which works well even if there is no pure pixel per endmember.These are explained below .

A.MVSA(Minimum volume simplex analysis)

This is a spectral unmixing algorithm which comes under the category of geometrical algorithms, and this is not a pure pixel based endmember extraction algorithm .i.e, this does not require an initial assumption that there should be atleast one pure pixel per endmember. This comes under the category of minimum volume based algorithms for spectral unmixing algorithm.This algorithm was put forward by J.Li in 2008 in[17] The mathematical and theoretical background of this algorithm is given below as explained in [17].

When coming to the mathematical part, we can start with the linear mixing model, which can be expressed follows

$$Y = Ms \qquad (1)$$
$$s.t \quad s \geq 0, 1_p^T S = 1_n^T$$

Where $Y = [y_1, y_2, ..., y_N] \in \mathbb{R}^{pXn}$ is the matrix holding in it's columns the spectral vectors $y_i \in \mathbb{R}^p$ for i=1,2,…,n of the hyperspectral data set under observation and $M = [m_1, m_2, ..., m_N] \in \mathbb{R}^{pXp}$ is the mixing matrix where m_i is the ith endmember and p represents the no. of endmembers considered., and $S \in \mathbb{R}^{pXn}$ denotes the abundance matrix containing the fractions. For each and every pixel ASC(abundance sum to one constraint),ANC((abundance nonnegativity constraint) should be satisfied. That is the abundance fraction vectors belong to probability simplex. By that reason, the spectral vectors y_i also belong to a simplex set with vertices m_i for i=1,..,N and the rest of the procedure is explained below.

Here Y is known for us and we have to find out the matrices M and S by fitting a minimum volume simplex to the data, according to the constraints shown in (1).This can be formulated in the form of following optimization problem.

$$M^* = \arg min_M \; |\det(M)|$$
$$s.t: \; QY \geq 0, \quad 1_P^T QY = 1 \qquad (2)$$

Where $Q = M^{-1}$ and since det(Q)=1/det(M) ,the problem in (2) can be modified as

$$Q^* = \arg max_Q \log |\det(Q)|$$
$$s.t \; QY \geq 0, 1_P^T \; QY = q_m \qquad (3)$$

The problems shown in (2) and(3) are purely non-linear ,even if the constraints are linear, and moreover the problem shown in(2) is nonconvex and it can have many local minima. By this reason we can not have an expectation of finding a global optima systematically.MVSA tries to find out a relatively good solution for it.

As a first step the set of constraints should be simplified, as shown here. $1_P^T QY = 1_N^T$ by assuming that each and every spectral vector y in the data set can be written as a linear combination of *p* linearly independent vectors taken from the hyperspectral data set $Y_p = [y_{i1}, y_{i2}, ..., y_{ip}]$,and ASC and ANC should be satisfied.ie, $y = Y_p \beta,$ whereas $1_p^T \beta = 1$ .It results in to ,the constraint $1_P^T QY = 1_N^T$ getting equal to $1_P^T QY_p = 1_N^T$ or else to $1_P^T Q = 1_p^T (Y_p)^{-1}$,and by this way defining $q_m = 1_p^T (Y_p)^{-1}$,it will lead to $1_P^T Q = q_m$. Thus considering all the above constraints the problem(3) got modified to

$$Q^* = \arg Max_Q \log |\det(Q)|$$
$$s.t \quad QY \geq 0, \; 1_p^T Q = q_m \qquad (4)$$

This optimization problem shown in equation (4) can be solved by finding the solution of the respective Kuhn-Tucker equations using sequential quadratic programming (SQP) methods which is a very efficient means for it.

To simplify the MVSA algorithm, it is initialized with the set of endmembers $M \equiv [m1, \ldots, mp]$ generated by the VCA . VCA[16] is chosen for this purpose because its is the fastest among all the pure pixel-based methods. The output of VCA is a set of *p* vectors that are in the data set, then all vectors belonging to the convex set generated by the columns of *M* are discarded. If the number of endmembers is large, it may happen that the initial simplex provided by VCA contains very few pixels inside and, therefore, most are outside, violating the nonnegativity constraints and slowing down the algorithm and error may occur. In such cases, the initial simplex is expanded to increase the number of pixels that are in the convex hull of the identified endmembers, which speeds up the algorithm and makes it more efficient.

If there exist some outliers and noise in the given data set, a final step is made to run in which the hard constraint $QY \geq 0$ is replaced by the soft constraint $-1^T hinge(-QY)1_n$ whereas hinge(*x*) is an element-wise operator that, for each component, yields the negative part of *x*. The optimization problem can be rewritten as shown below

$$Q^* = \arg Max_Q \log|\det(Q)| - \lambda 1^T hinge(QY)1_n \qquad (5)$$
$$s.t \quad 1_p^T Q = q_m$$

where λ term controls the relative weight between the soft constraint and the the log | det(Q)| term. Important point is that , this soft constraint gives zero weight to nonnegative abundance fractions and negative weight to negative abundance fractions. In this way there is slack for the abundance fractions originated in outliers or noise to be negative. To solve problem (5), SQP is again applied to the new objective function, but the inequality constraint is removed.

$$Q := \mathrm{SQP}(f_{soft}, Q_0, A_{eq}, b_{eq}, g, H)$$

B.MVES(Minimum Volume Enclosing Simplex)

Minimum volume enclosing simplex analysis is another efficient spectral unmixing algorithm which comes under geometrical algorithms. Like MVSA algorithm, this is also a non pure pixel based algorithm and works on the basis of minimum volume assumption. The details of the algorithm is explained below as in[18].

The problem of MVES is entirely based on the convex hull and using that the problem can be written as follows.

$$\min_{\beta_1,\ldots,\beta_N} V(\beta_1,\ldots,\beta_N) \quad (1)$$
$$s.t\ \tilde{x}[n] \in conv\{\beta_1,\ldots,\beta_N\}, \forall n$$

Where

$$V(\beta_1,\ldots,\beta_N) = \frac{|\det(\Delta(\beta_1,\ldots,\beta_N))|}{(N-1)!} \quad (2)$$

Whereas $V(\beta_1,\ldots,\beta_N)$ is the volume of the simplex $conv\{\beta_1,\ldots,\beta_N\} \subset \mathbb{R}^{N-1}$ and in the equation (2)

$$\Delta(\beta_1,\ldots,\beta_N) = \begin{bmatrix} \beta_1 \ldots\ldots\ldots \beta_N \\ 1 \ldots\ldots\ldots\ldots 1 \end{bmatrix} \quad (3)$$

An alternative expression shown in (1) can be expressed as shown below.

$$V(\beta_1,\ldots,\beta_N) = \frac{|\det(B)|}{(N-1)!} \quad (4)$$

Where

$$B = [\beta_1 - \beta_N, \ldots, \beta_{N-1}, \beta_N] \in \mathbb{R}^{(N-1)X(N-1)} \quad (5)$$

In addition to that,any dimension reduced pixel $\tilde{x}[n] \in conv\{\beta_1,\ldots,\beta_N\}$ can be expressed as

$$\tilde{x}[n] = \sum_{i=1}^{N} s_i[n]\beta_i = \beta_N + Bs'[n] \quad (6)$$

Where

$$s'[n] = (s_1[n],\ldots,s_{N-1}[n])^T \geq 0 \ \&\ s_N[n] = 1 - 1_{N-1}^T s'[n] \geq 0$$

and by this reason the problem in (1) can be written as

$$\min_{B,\beta_N,\ s'[1],\ldots,s'[L]} |\det(B)| \quad (7a)$$
$$s.t\quad s'[n] \geq 0, 1_{N-1}^T s'[n] \leq 1 \quad (7b)$$
$$\tilde{x}[n] = \beta_N + Bs'[n] \quad \forall n = 1,\ldots,L \quad (7c)$$

The problem shown in (7) is a nonconvex one and while the nonconvexity of the objective function is an obstacle, at the same time the nonlinear equality constraints in (7c) impose difficulty for solving the problem. A modified version of (7) is given below in which the original nonconvex constraints are transformed into convex constraints and makes it more easy to solve. Here one to one mappings of the optimization variables are considered

$$H = B^{-1} \in \mathbb{R}^{(N-1)X(N-1)} \quad (8a)$$
$$g = B^{-1}\beta_N \in \mathbb{R}^{(N-1)} \quad (8b)$$

Then $s'[n]$ can be expressed as follows

$$s'[n] = B^{-1}(\tilde{x}[n] - \beta_N) = H\tilde{x}[n] - g \quad (9)$$

Substituting the above equations (8) and (9) in to equation shown in(7),the equivalent problem is obtained as

$$\max_{H,g} |\det(H)| \quad (10)$$
$$s.t\quad H\tilde{x}[n] - g \geq 0$$
$$1_{N-1}^T(H\tilde{x}[n] - g) \leq 1, \forall n = 1,\ldots,L$$

In the above equation (10) all the constraints are linear and convex. The MVES problem shown in (10) has a convex feasible set, but its objective is still nonconvex and this makes problem more difficult. Moreover the structure of problem (10) provide an opportunity to use the efficient Linear Programming to solve the problem. The cofactor expansion for |det(H)| is as follows.

$$\det(H) = \sum_{j=1}^{N-1} (-1)^{i+j} h_{ij} \det(H_{ij}) \quad (11)$$

As by this for any i=1,…..,N-1 where h_{ij} is the (i,j)th entry of H, and $H_{ij} \in \mathbb{R}^{(N-2)X(N-2)}$ is a submatrix of H with the ith row and jth column removed from the matrix. It should be noted that with a fixed H_{ij} ,det(H) is a linear function of h_{ij}, with j=1,2…N-1. Then consider updating one row vector of H and one entry of g where fixing the other rows of H and the other entries of g inorder to solve the problem . Then now it can be denote h_i^T the ith row vector of H , and g_i denote the ith entry of g . The partial maximization of problem shown in (10) with respect to h_i and g_i is given by

$$\max_{h_i^T, g_i} \left| \sum_{j=1}^{N-1} (-1)^{i+j} h_{ij} \det(H_{ij}) \right| \quad (12)$$
$$s.t\quad 0 \leq h_i^T \tilde{x}[n] - g_i \leq 1 - \sum_{j \neq 1} (h_{ij}^T \tilde{x}[n] - g_j)$$

It can be seen that the objective function of the problem in (12) is nonconvex still this moment. Then it can solved only by breaking it in to two LPs as below

$$p^* = \max_{h_i^T, g_i} \sum_{j=1}^{N-1} (-1)^{i+j} h_{ij} \det(H_{ij}) \quad (13)$$
$$s.t \quad 0 \le h_i^T \tilde{x}[n] - g_i \le 1 - \sum_{j \ne 1} (h_j^T \tilde{x}[n] - g_j) \quad \forall n$$

$$q^* = \min_{h_i^T, g_i} \sum_{j=1}^{N-1} (-1)^{i+j} h_{ij} \det(H_{ij}) \quad (14)$$
$$s.t \quad 0 \le h_i^T \tilde{x}[n] - g_i \le 1 - \sum_{j \ne 1} (h_j^T \tilde{x}[n] - g_j) \quad \forall n$$

The optimal solution of problem shown in(12) denoted by $((h_i^T)^*, g_i^*)$ is opted as the solution of (13) if $|p^*| > |q^*|$,and the solution of (14) if $|q^*| > |p^*|$ .This type of row-wise minimization process is done cyclically until stopping condition is met. After finding out (H^*, g^*) ,the dimension reduced endmembers $\hat{\alpha}_1, ..., \hat{\alpha}_N$ are found out by

$$\hat{\alpha}_N = (H^*)^{-1} g^* \quad (15)$$

$$[\hat{\alpha}_1 ....., \hat{\alpha}_{N-1}] = \hat{\alpha}_N 1_{N-1}^T + (H^*)^{-1} \quad (16)$$

Then the endmember signature estimates can be obtained as $\hat{a}_i = C\hat{\alpha}_i + d$ for i=1,…..,N. Then the abundance vectors can be obtained without inversion as follows

$$\hat{s}[n] = [s'[n]^T \quad 1 - 1_{N-1}^T s'[n]]^T$$
$$= [(H^* \tilde{x}[n] - g^*)^T \quad 1 - 1_{N-1}^T (H^* \tilde{x}[n] - g^*)]^T \ \forall n \ (17)$$

Thus MVES solves the problem of spectral unmixing problem and finds out endmember estimates and abundance maps simultaneously without using any other inversion process[18].

C.SISAL(simplex identification via split and augmented lagrangian)

This is another popularly used spectral unmixing algorithm which comes under the category of minimum volume based geometrical approaches put forward by J.M.Biouscas. This is explained as follows as in[19] and mathematical explanation is also taken from[19].

First in this case take that there are p endmembers, with spectral signatures $m_i \in \square^l$, for i=1,…,p, where $l \ge p$ denotes the number of spectral bands for that sensor. Under the linear mixing model, a hyperspectral vector observed is a linear combination of the endmember signatures, where the weights represent the fractions that each endmember occupies in each pixel.

Let $Y \equiv [y_1, \ldots, y_n] \in \square^{l \times n}$ denote a matrix containing the observed spectral vectors of the scene $y_i \in \square^l$ and $S \equiv [s_1, \ldots, s_n] \in \square^{p \times n}$ a matrix containing respective fractions; i.e., $y_i = Ms_i$, for i=1,..,n, where $M \equiv [m_1, \ldots, m_p] \in \square^{p \times p}$ is the mixing matrix containing the endmembers of the observed scene, and s_i is a vector indicating the fractions, called as fractional abundances. Due to the reason that the components of s_i are nonnegative and sum to one then the fractional abundance vectors belong to the standard set as shown below. $S_p = \{ s \in \square^p : s \ge 0, 1_p^T s = 1 \}^1$. By this the linear model can be shown as

$$Y = MS, \ S \in S_p^n. \quad (1)$$

In this algorithm implementation , it was assumed initially that the number of endmembers and signal subspace is known before and that the observed vectors y_i, i=1,…,n, represent coordinates with respect to a p-dimensional basis of the signal subspace formed by the spectral vectors.

In this the job was to estimate matrices M and S by fitting a minimum volume simplex to the hyperspectral data subject to the constraints S≥0 and $1_p^T S = 1_n$. Due to the reason that the volume defined by the columns of M is proportional to |det(M) | then it can written as

$$M^* = \arg \min_M |\det(M)|$$
$$s.t. : QY \ge 0, \ 1_p^T QY = 1_n^T \quad (2)$$

where $Q = M^{-1}$. Since det(Q)=1/det(M), the problem (2) is replaced with

$$Q^* = \arg \min_Q -\log|\det(Q)|$$
$$s.t. : QY \ge 0, \ 1_p^T QY = 1_n^T \quad (3)$$

It can be seen that constraints in (3) also define a convex set. If the matrix Q is symmetric and positive-definite, then the problem (3) is convex and thus it should be solved in that way. But in many cases Q is neither symmetric nor positive-definite and, thus the problem (3) becomes a nonconvex one. So global optima of (3) can not be found. By the SISAL algorithm introduced by J.M Biouscas in [123] can provide nice sub-optimal solutions for this.

The set of constraints are simplified as follows as the first step. $1_p^T QY = 1_n^T$ First it is noted that the vector 1_n^T does not belong to the null space of Y matrix observed. In other way , the null vector should belong to the affine hull of mixing matrix M, and that imply that the columns of M would not be independent. So, by multiplying the equality constraint on the right hand side by $Y^T (YY^T)^{-1}$, it will be as, $(1_p^T QY = 1_n^T) \Leftrightarrow (1_p^T Q = a^T)$ where $a^T \equiv 1_n Y^T (YY^T)^{-1}$.

Then the problem shown in (3got modified to,

$$Q^* = \arg \min_Q -\log|\det(Q)|$$
$$s.t. : QY \ge 0, \ 1_p^T Q = a^T \quad (4)$$

For getting the solution solve the following modified version:

$$Q^* = \arg \min_Q -\log|\det(Q)| + \lambda \|QY\|_h$$
$$s.t. : 1_p^T Q = a^T \quad (5)$$

where $\|x\|_h \equiv \sum_{ij} h(|x|_{ij})$ and $h(x) \equiv \max\{-x, 0\}$ is the hinge function which is a modified version shown in[123]. The amount of regularization is controlled mainly by the regularization parameter term $\lambda > 0$. ,By replacing $n \times p$ equality constraints by a regularizer, it deals with large scale problems.The following is the explanation of how is the sequence of a convex problem goes.

Let $q \equiv vec(Q)$ denotes an operator that stacks the columns of Q in the column vector q. It is given that $vec(AB) = (B^T \otimes I) vec(A) = (I \otimes A) vec(B)$ where "⊗" denotes the kronecker operator, and by defining $f(q) = -\log|\det(Q)|$, then the equation (5) can be rewritten as

$$q^* = \arg\min_q f(q) + \lambda \|Aq\|_h$$
$$\text{s.t. : } Bq=a, \qquad (6)$$

where $A = (Y^T \otimes I)$ and $B = (I \otimes 1_p^T)$. Thus the Hessian of f is defined as $H = K_n |Q^{-T} \otimes Q^{-1}|$, where K_n is the comutation matrix $(\text{i.e., } K_n \text{vec}(A) = \text{vec}(A^T))$. Using a quadratic approximation for f(q), the problem shown in (6) is approximated by computing a descent sequence $q_k, k = 0,1,...,$ with the following algorithm shown in steps:

Algorithm 1

1. Set k=0, choose $\mu > 0$ and $q_0 = \text{VCA}(Y)$.
2. repeat
3. $l_k = f(q_k) + \lambda \|Aq_k\|_h$
4. $g = -\text{vec}(Q^{-1})$
5. $q_{k+1} \in \arg\min_q g^T q + \mu \|q - q_k\|^2 + \lambda \|Aq\|_h$
6. s.t.: $Bq = a$
7. if $f(q_{k+1}) + \lambda \|Aq_{k+1}\|_h > l_k$
8. find $q \in \{\alpha q_{k+1} + (1-\alpha) q_k : 0 < \alpha < 1\}$
9. such that $f(q) + \lambda \|Aq\|_h \le l_k$
10. $q_{k+1} = q$
11. $k \leftarrow k+1$
12. until a stopping criterion is satisfied.

This algorithm shown above is initialized with the VCA estimate as in MVSA algorithm. Step 4 computes the gradient of f(q) and step 5 minimizes a strictly convex approximation to the initial objective function, and here the term f(q) was replaced by a quadratic approximation. It should be noted that the term $\|q_{k+1} - q_k\|^2$ does not grow unbounded. Inorder to solve the minimization in steps 5-6, in the next subsection a variable splitting augmented Lagrangian algorithm was introduced by the author of [19].

The optimization problem of steps 5-6 of Algorithm 1 is written as

$$\min_{q,z} E(q,z)$$
$$\text{s.t. : } Bq = a, Aq = z, \qquad (7)$$

where $E(q,z) \equiv g^T q + \mu \|q - q_k\|^2 + \lambda \|z\|_h$

In equation (7), the variable q was found as splitted into the pair (q,z) and got linked through the constraint Aq=z. The augmented Lagrangian (AL) for this problem, is shown as

$$\varsigma(q,z,d,\tau) \equiv E(q,z) + \alpha^T (Aq - z) + \tau \|Aq - z\|^2 \qquad (8)$$
$$= E(q,z) + \tau \|Aq - z - d\|^2 + c, \qquad (9)$$

where α holds the Lagrangian multipliers, $d = -\alpha/(2\tau)$, and c is an irrelevant constant in this problem. The Augmented Lagrangian algorithm consists in minimizing ς with respect to (q,z) and then updating α,which is given as follows in[19]. The algorithm 2 shown below opens door to the final stage of the SISAL algorithm.

Algorithm 2 Augmented Lagrangian Algorithm

1. Set t=0, choose (q_0, z_0), α_0 and $\tau > 0$,
2. repeat
3. $(q_{t+1}, z_{t+1}) \in \arg\min_z \varsigma(q, z, d, \tau)$
4. s.t.: $Bq = a$
5. $d_{t+1} \leftarrow d_t - (Aq_{t+1} - z_{t+1})$
6. $t \leftarrow t+1$
7. until a stopping criterion is satisfied.

The exact solution of the optimization with respect to (q,z) in the step 3 of the Algorithm 2 is really a tough problem. But , the block minimizations with respect to q and with respect to z are easy to find out. Based on this, In [123] author proposed the following modified version of algorithm 2 shown above:

Algorithm 3 Alternating Split AL

1. Set t=0, choose (q_0, z_0), α_0 and $\tau > 0$,
2. repeat
3. $q_{t+1} \in \arg\min_q g^T q + \frac{\mu}{2}\|q - q_k\|^2 + \frac{\mu}{2}\|Aq - z_t - d_t\|^2$
4. s.t.: $Bq = a$
5. $z_{t+1} \in \arg\min_z \frac{1}{2}\|Aq_{t+1} - z - d_t\|^2 + \frac{\lambda}{\tau}\|z\|_h$
6. $d_{t+1} \leftarrow d_t - (Aq_{t+1} - z_{t+1})$
7. $t \leftarrow t+1$
8. until a stopping criterion is satisfied.

The quadratic problem with linear constraints in steps 3-4 is solved and solution is given as follows

$$q_{t+1} = F^{-1}b - F^{-1}B^T (BF^{-1}B^T)^{-1} (BF^{-1}b - a), \qquad (10)$$

Where

$$F = (\mu I + \tau A^T A)$$
$$b = \mu q_t - g + \tau A^T (z_t + d_t). \qquad (11)$$

Thus SISAL[19] efficiently solves the problem of spectral unmixing and this represents a modified version of MVSA algorithm for spectral unmixing.

III. EXPERIMENTAL DETAILS , RESULTS & ANALYSIS

In this section the experimental details, results and performance analysis of the three algorithms namely MVSA,MVES and SISAL on the real hyperspectral dataset cuprite data taken over Nevada, U.S in 1997[20] is done.The three geometrical minimum volume based algorithms are applied to this hyperspectral dataset for performing spectral unmixing of the acquired scene. Only a subimage of the hyperspectral data is taken as a region of interest for reducing the computational complexity, which is of size 250x191 pixels(L=47750).This contains 224 spectral bands over the wavelength region of 0.4μm to 2.5 μm. As the first step, we should get a knowledge about, how many endmembers(pure reference materials) are there in this region of interest of 250x191 pixels. For this Hyperspectral subspace identification by minimum error (HySime) [21] is applied to this dataset and thus it was found that the number of endmembers located in this region is N=18.In this dataset, the bands 1-2,104-113,148-167 and 221-224 were removed from this , due to low SNR effect which occurs due to the effect of water vapour and atmospheric effects and this may reduce the performance if not removed. Thus the now current dataset contains 188 spectral bands instead of 224 bands . The abundance maps corresponding to each mineral or

endmember were obtained and shown in fig 4. The minerals detected by the spectral unmixing process was identified by the visual comparison of the abundance maps obtained as the output with the abundance maps results given in [22],[23],[24]and[25].

Spectral unmixing will give spectral signatures of endmembers and also their corresponding abundance maps as outputs of this process in the given dataset. Here in this paper the metric used for the evaluation of results is Spectral Angle Mapper (SAM)[26] which provides accurate results of evaluation. It's measured between the original library spectra which is obtained from U.S.G.S spectral library [27], and the spectra obtained as the output by the spectral unmixing process by various algorithms . The basic equation for the spectral angle mapper is shown as follows in [26].

$$\theta(x, y) = \arccos\left(\frac{(< x, y >)}{\|x\|\|y\|}\right)$$

Where, x is the reference library spectra from U.S.G.S library and y is the spectra of minerals obtained from spectral unmixing in this case. As the value of spectral angle score decreases, the result becomes more accurate and when it gains a high value for SA we can conclude that the performance of algorithm is poor[26]. The values of SA scores for all the estimated endmembers obtained by all the 3 algorithms mentioned is given in Table1.The similarity scores which are put in parentheses denote the value of SA for the estimated endmember which is repeated . Due to the space limit here it is shown the estimated endmember spectral signatures and corresponding abundance maps of SISAL algorithm only. In this repeated mineral maps and signatures are avoided due to space limit. The abundance maps and spectral signatures are shown below in Fig 4 and Fig 5.

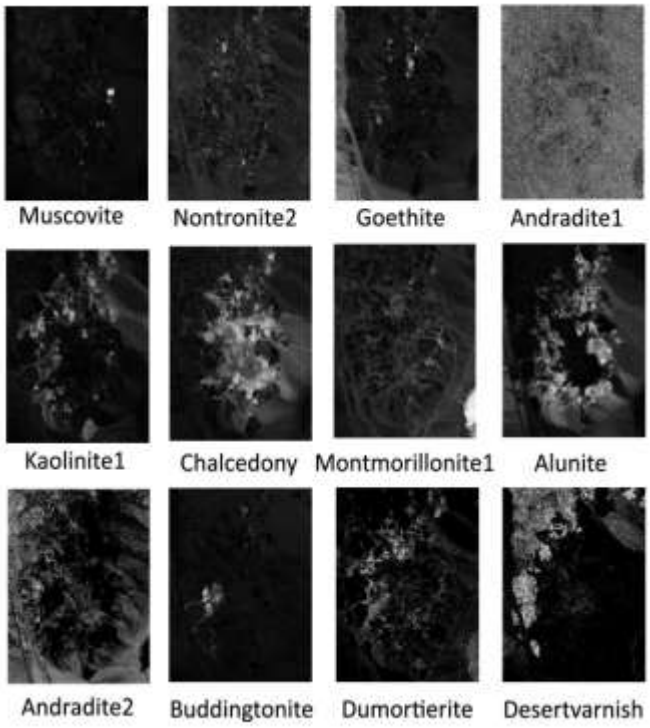

Fig 4.Abundance maps estimated by SISAL algorithm

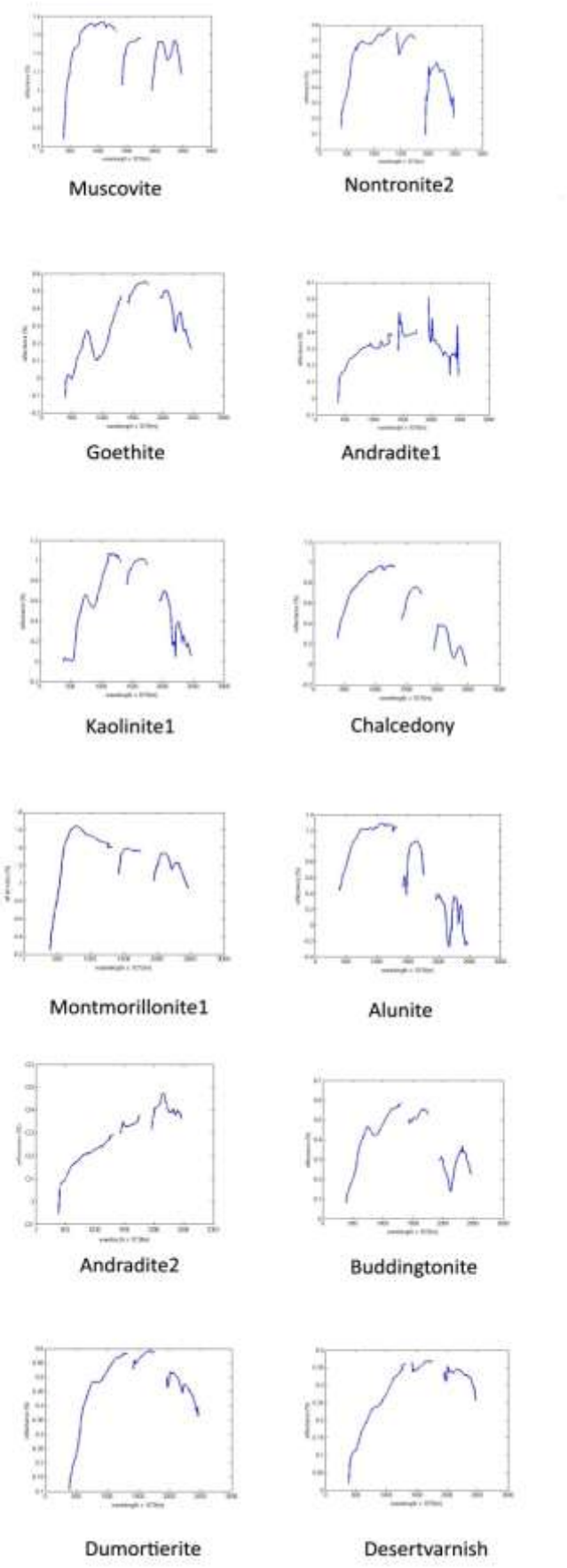

Fig.5.Spectral signatures estimated by SISAL algorithm

Table 1.Spectral angle scores for MVSA,MVES and SISAL algorithms.

MINERALS	MVES	SISAL	MVSA
1)Buddingtonite	-	10.03	-
2)Nontronite2	-	10.40 (11.16) (10.77)	-
3)Kaolinite1	10.04 (25.69) (21.49)	24.07	21.98 (21.74) (22.40)
4)Kaolinite2	16.52 (13.85)	-	27.38
5)Muscovite	9.86	9.58 (11.19)	10.17
6)Dumortierite	16.96 (13.13)	7.63	14.73 (19.84) (17.40)
7)Desertvarnish	-	6.07	-
8)Alunite	10.54 (10.19) (20.49) (12.76) (10.12)	15.81	9.75 (9.04) (11.35) (8.44)
9)Chalcedony	-	19.42 (6.48)	13.73
10)Montmorillonite1	7.83 (5.23) (5.18) (6.09) (8.42)	7.66	5.16 (7.89) (6.16) (5.54) (5.64)
11)Goethite	-	11.74	-
12)Andradite1	-	9.52 (12.15) (11.09)	-
13)Andradite2	-	8.11	-
Average SA	12.46	11.25	13.24

The table 1 shown above gives the spectral similarity scores of the three algorithms mentioned as MVSA, MVES and SISAL.

In many hyperspectral data sets where the data is highly mixed the pure pixel assumption will not be satisfied .i.e there will not be a pure pixel existing for each endmember. At this situation These algorithms comes to play and helps the users to perform spectral unmixing without pure pixels.

All the algorithms in this type adopt a minimum volume condition aimed at finding the endmember matrix M by minimizing the volume of the simplex defined by its columns and containing the endmembers of the scene observed. This is a nonconvex optimization problem

The SA similarity values are measured with reference to U.S.G.S spectral library (available online). When analyzing the table it can be seen that, out of 3 algorithms, Average SA is high for MVSA(Minimum volume simplex analysis). This gains a value of Average SA as 13.24 .This indicates the poor performance of MVSA algorithm compared to other 2 spectral unmixing algorithms. In the set of 3 algorithms ,SISAL gives good performance when compared to all the other two algorithms with an average SA score of 11.25.Then MVES(Minimum Volume Enclosing Simplex) comes after SISAL with an average SA of 12.46. Then MVSA (Minimum volume simplex analysis) comes to the third place with an average SA of 13.24 (Note that all these SA values are measured in degrees.).

In the case of MVSA and SISAL algorithms carries a robust version of the minimum volume concept. But in SISAL, the positivity hard constraints are replaced by hinge type soft constraints, whose strength is controlled by a regularization parameter λ and thus proceeds the algorithm. This replacement of hard constraints is having three main advantages: 1) This offers robustness to poor initialization 2) Provides robustness to outliers and noise in the dataset ; 3) This gives a way for dealing with large problems. Moreover , for large values of the regularization parameter, the hard constraint formulation is recovered. Inoredrto overcome the hard nonconvex optimization problem in this method a sequence of nonsmooth convex subproblems is solved , using variable splitting to obtain a constraint formulation, and then applying an augmented Lagrangian technique .This sub-problems implement an alternate minimization scheme, with very simple and fast steps and by all these reasons SISAL can give good results when compared to all the 2 algorithms.MVSA and MVES are not bad in their performance. In this performance analysis of three minimum volume based algorithms, it can be seen that all the three minimum volume based geometrical approaches give good results for spectral unmixing. There is only a difference of 1 degree in the score of average spectral angle as shown in the table 1.

IV. Conclusion

In this paper ,performance analysis and comparative study of 3 non- pure pixel,minimum based geometrical algorithms namely MVSA(Minimum volume simplex analysis),SISAL(Simplex identification via splitted and augmented lagrangian) and MVES(Minimum volume enclosing simplex) is done. All the 3 algorithms are applied on the real hyperspectral dataset , AVIRIS CUPRITE data taken over NEVADA,U.S in 1997. The metric used for the validation of all the algorithms is SAM(Spectral angle mapper).This is measured in degrees between the original library spectra from U.S.G.S spectral library and the spectra obtained by spectral unmixing by various algorithms. Thus the performance evaluation of all 3 algorithms is done and it is found that SISAL gives better result compared to other 2 algorithms as MVSA and MVES but only b .

As a work in future different spectral unmixing algorithms coming under sparse and geometrical approaches can be

included in the studies and more comparative studies can be done with statistical and sparse approaches.

ACKNOWLEDGMENT

The authors of this paper wish to sincerely thank Dr.J.M Biouscas for his valuable comments and suggestions in this work and implementation of codes, and Dr.Tsung –Han Chan for the suggestions in this work.Authors are also thankful to Dr.K.A narayanankutty for his help in this work.

REFERENCES

[1] G.Shaw and D.Manolakis "*signal processing for hyperspectral image exploitation*,"IEEE SIGNAL Process.Mag ,.vol 19,no.1,pp,12-16,jan 2002

[2] T.Lillesand and R.kiefer,"*Remote sensing and interpretation*",3rd ed.Newyork:Wiley,1994.

[3] R.O Green,M.L.Eastwood,C.M Sarture,T.G Chrien,M.arosson,B.J Chippendale,J.A .Faust ,B.E .Pavri,C.J .Chovit,and MSoils et al.,"*Imaging spectroscopy and the airborne visible/infrared imaging spectrometer(AVIRIS*),"RemoteSens.Environ.,vol.65.no3,pp,227-248, 1998

[4] N.Keshava," *A Survey of Spectral unmixing algorithms*"Lincoln Laboratory journal, vol 14, November 2003

[5] Websitehttp://www.sed.manchester.ac.uk/geography/research/uperu/project4.htm

[6] J.Settle and N.Drake."*Linear mixing and the estmation of ground cover proportions*,"Int.J.RemoteSens.,vol.14.no.6.pp.11591177,Apr 1993

[7] C.Borel and S.Gerstl," *Nonlinear spectral mixing model for vegetative and soil surfaces*."Remote Sens.Environ.,vol 47,no.3,pp.403-416,Mar.1994

[8] M.D .Iordache,J.Biouscas, and A.plaza , "*Sparse unmixing of hyperspectraldata*,",IEEETrans.Geosci.Remotesen.vol.49,no.6,pp.20 14 -2039,2011.

[9] Jose.M.BiouscasDias,AntonioPlaza,NicolasDobigeon,MarioParente, Qian Du,Paul Gader,Jocelyn Chanussot,"*Hyperspectral Unmixing Overview:Geometrical ,statistical,and Sparse Regression –Based Approaches*."IEEE journal of selected topics in applied earth observations and remotesensing,vol.5.No2.April 2012

[10] J.Nascimento and J.Biouscas Dias "*Does Independent component analysis playa role in unmixing hyperspectral data?,"*IEEE Trans.Geosci.Remote sens.vol43.no.1.pp.175-187,2005 .

[11] J.M.P .Nascimento and J.M Biouscas dias "*Hyperspectral unmixing algorithm via dependent component analysis*"in proc.IEEE Int.conf.Geosci.Remote sensing.vol50,no.3,pp.863-878,2012 .

[12] Marian-Daniel Iordache,Jose.M.Biouscas,and Antonio-plaza,"*Total variation spatial regularization for sparse hyperspectral unmixing*"IEEE Trans.Geosci.Remote sens.,April2012

[13] T.H chan, W.K Ma, A.Ambikapathi,and C.Y .Chi,"*A simplex volume Maximization framework for hyperspectral endmember extraction algorithm,*"IEEE Trans.Geosci.Remote Sens.vol49, no.11, 2011.

[14] T.H chan, W.K Ma, A.Ambikapathi, and C.Y .Chi "*Robust Affine set Fitting and Fast simplexVolume Max-Min for Hyperspectral Endmember Extraction*."IEEE trans.Geosci.Remote Sensing.

[15] M.E Winter,"N-Findr :An algorithm for fast autonomous spectral endmember determination in hyperspectral data,"in proc.SPIE image Spectrometry V,1999,vol.3753, pp.266-277.

[16] J.M.P Nascimento and J.M.Biouscas,"*Vertex component analysis: A fast algorithm to unmix hyperspectral data*,"IEE Trans. Geos.Remote Sens.vol.43.no 4.pp,898-910,2005

[17] J.Li and J.Biouscas-Dias ,"*Minimum volume simplex analysis:A fast algorithm to unmix hyperspectral data*,"in proc.IEEE Int.Conf.Geosci.Remote sens.(IGARSS)2008,VOL.3,PP.250-253

[18] T.Chan,C.Chi,Y.Huang ,and W.ma,"*Convex analysis based minimum volume enclosing simplex algorithm for hyperspectral unmixing*," IEEE Trans.Signal Process.,Vol57,no.11,pp,4418-4432,2009

[19] J.M Biouscas Dias,"A variable splitting and augmented lagrangian approach to linear spectral unmixing."in proc.IEEE GRSS workshop Hyperspectral Image process. Vol57, no.11, pp,4418-4432, 2009,pp.1-4

[20] AVIRIS Free Standard Data products.[online]Available:http://aviris.Jpl.nasa.gov/html/aviris.freedata.html

[21] J.M Biouscas-Dias and J.M.P Nascimento,"*Hyperspectral subspace identification*,"IEEE Trans.Geosci.Remote sens..vol46.no.8.pp.2435-2445, aug2008

[22] L.Miao and H.Qi,"*Endmember extraction from highly mixed data using minimum volume constrained nonnegative matrix factoriza tion*".IEEE Trans.Geosci.Remote sens.vol45,no.3,pp.765-777,2007

[23]A.Ambikapathi, T.H Chan, W.k ma, and C.Y chi,"*Chance constrained Robust minimum volume enclosing simplex algorithm for hyper Spectral unmixing,"*IEEE Trans.Geosci.remote Sens.Vol.49, no.11, Pp, 4194-4209, Nov-2011

[24] Nascimento,J.M.P.(2006*)," Unsupervised unmixing*" Doctoral dissertation,universidade Technica de lisboa

[25] G. Swayze, R. Clark, S. Sutley, and A. Gallagher, "*Ground-truthing AVIRIS mineral mapping at Cuprite, Nevada*," in *Proc. Summer 4th Annu. JPL Airborne Geosci. Workshop*, 1992, vol. 2, pp. 47–49.

[26] N.Keshava,"*Distance metrics and Band selection in hyperspectral Processing with applications to material identification and spectral libraries*,"project report HTAP-R Lincoln laboratorydec2002.

[27] Tech.Rep.[Online].Available:http://speclab.cr.usgs.gov/cuprite.html